

## Optical design for a bending-magnet beamline based on a varied-line-spacing plane grating

Takanori Kiyokura,\* Fumihiko Maeda and Yoshio Watanabe

NTT Basic Research Laboratories, 3-1 Morinosato Wakamiya, Atsugi-shi, Kanagawa 243-0198, Japan.  
E-mail: kiyokura@will.brl.ntt.co.jp

(Received 4 August 1997; accepted 18 November 1997)

A vacuum ultraviolet beamline with a grazing-incidence constant-deviation-angle monochromator, equipped with a varied-line-spacing plane grating, has been designed for a bending-magnet light source. This type of monochromator has become very popular because of its high resolution, high throughput, simple scanning mechanism and fixed exit slit. To improve the energy resolution for a wide spectral range, Yan & Yagishita [(1995), KEK Report 95-9. KEK, Tsukuba, Ibaraki 305, Japan] proposed eliminating the defocus aberration at two specific energies in the spectral range, and their monochromator successfully achieved higher energy resolution by using an undulator light source. The possibility of applying this method to a bending-magnet beamline was examined and it was found that high performance can be achieved even using a bending-magnet light source with wide emittance. Performance evaluation relating to energy resolution, photon flux and spot size are reported.

**Keywords:** bending-magnet beamlines; high resolution; monochromators; varied-line-spacing plane gratings.

### 1. Introduction

Recently, constant-deviation-angle varied-line-spacing plane-grating (VLSPG) monochromators (Koike *et al.*, 1994; Amemiya *et al.*, 1996) have become very popular because of their high resolution, high throughput, simple scanning mechanism and fixed exit slit. However, since the VLSPG monochromator is usually designed to eliminate the defocus aberration at one energy, high resolution cannot be obtained at energies other than the optimized one. To decrease the defocus aberration over a wide spectral range, Yan & Yagishita (1995) and Hettrick & Underwood (1988) proposed eliminating the defocus aberration at two specific energies in the spectral range, and their monochromator successfully achieved high resolution by using an undulator light source. In the case of using a bending-magnet light source, it was thought to be difficult to achieve both high-energy resolution and high throughput because of the wide emittance at the source. In this paper we examine the possibility of applying this method to a bending-magnet beamline. We show that an energy resolution of  $10^{-4}$  and a photon flux of  $10^{11}$  photons  $s^{-1}$  can be achieved even using a wide-emittance bending-magnet light source.

### 2. Optical design

Our goal for this beamline design was to gain photon flux as efficiently as possible at an energy resolution of  $10^{-4}$  over the full spectral range (20–240 eV) for the study of solid surface chemical states and electronic properties.

We assumed the optical element layout of the beamline as shown in Fig. 1. The light source parameters are given in Table 1.

The acceptance angle of the beamline was set to 5 mrad (horizontal)  $\times$  2.5 mrad (vertical) by an aperture located 6 m from the light source. The first mirror of the beamline, *M0*, is a toroidal mirror with a  $5^\circ$  grazing incidence; it deflects light horizontally by  $10^\circ$  and focuses the light on the entrance slit along the vertical direction. The light is also focused along the horizontal direction at the midpoint between mirror *M1* and the grating to avoid astigmatism on *M1* and the grating. The second mirror, *M1*, is a spherical mirror with a  $4^\circ$  grazing incidence, and light is deflected vertically by  $8^\circ$ . It was designed to focus light on the exit slit with a magnification of unity to avoid coma aberration. *M1* also forms a convergent beam for the plane grating. After *M1*, the white light is diffracted by the grating and the selected wavelength is focused on the exit slit. Three interchangeable gratings, *GA*, *GB* and *GC*, with groove densities of 300, 600 and 1200 lines  $mm^{-1}$ , are used to cover efficiently the entire spectral range. The spectral ranges for *GA*, *GB* and *GC* were set to be 20–60, 40–120 and 80–240 eV, respectively. The deflection angle of the grating is  $165^\circ$ . The monochromated light is then refocused onto the sample by toroidal mirror *M2* with a magnification of unity, the direction of the light returning to parallel to the horizontal plane by *M2*, with a  $3.5^\circ$  grazing incidence.

The VLSPG is designed to correct optical aberrations using the light-path function method (Harada & Kita, 1980). The defocus aberration is most severe for degrading the energy resolution because of the fixed exit slit. The defocus aberration term of the light-path function of the VLSPG,  $F_{20}$ , is expressed as

$$F_{20}(b_2) = \cos^2 \alpha / r + \cos^2 \beta / r' + b_2 m \lambda / d_0. \quad (1)$$

The varied-line-spacing parameters are defined as

$$d(w) = d_0 / (1 + 2b_2 w + 3b_3 w^2 + 4b_4 w^3), \quad (2)$$

where  $\alpha$  and  $\beta$  are the incidence and diffraction angles, respectively,  $r$  is the entrance arm length,  $r'$  is the exit arm length,  $w$  is the coordinate along the grating,  $d(w)$  is the line spacing at the coordinate  $w$ ,  $d_0$  is the line spacing at the grating centre, which equals  $d(0)$ ,  $m$  is the diffraction order, and  $b_2$ ,  $b_3$  and  $b_4$  are the varied-line-spacing parameters to correct the defocus aberration, coma aberration and spherical aberration, respectively.

Usually,  $b_2$  is obtained from the equation  $F_{20} = 0$ , because parameter  $b_2$  is optimized at one energy in the spectral range. However, because defocus aberration remains at the low-energy

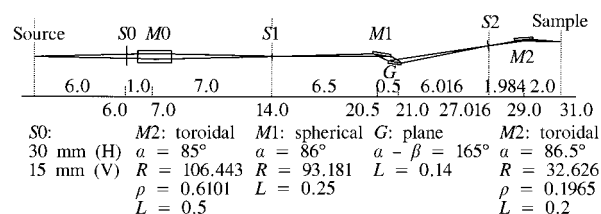


**Figure 1**  
Optical layout of the beamline (side view).

**Table 1**  
Parameters for the bending-magnet light source.

Parameter	Value
Nominal electron energy	2.5 GeV
Stored current	300 mA
Horizontal source size	0.366 mm
Vertical source size	0.052 mm
Horizontal source divergence	0.073 mrad
Vertical source divergence	0.011 mrad
Bending radius	8.66 m

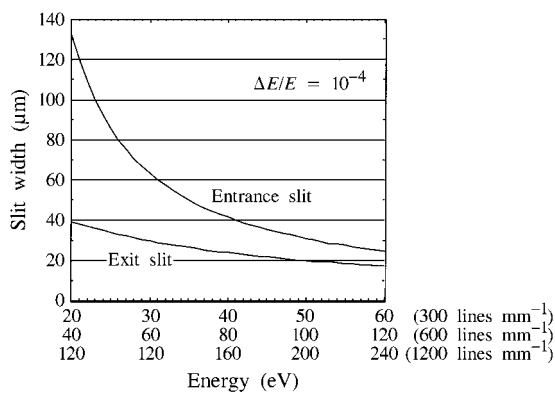
edge and the high-energy edge of the spectral range, these large defocus aberrations degrade the energy resolution in this spectral range. To decrease the defocus aberration over the full spectral range, Yan & Yagishita (1995) proposed a design method in which the defocus aberration vanishes at two specific energies in the spectral range. In this method, two wavelengths,  $\lambda_1$  and  $\lambda_2$ , are selected and the simultaneous equations of  $F_{20}(\lambda_1, b_2, r') = 0$  and  $F_{20}(\lambda_2, b_2, r') = 0$  are solved. Then the varied-line-spacing parameter,  $b_2$ , and the exit arm length,  $r'$ , were obtained. By diminishing the defocus aberration at two wavelengths, we decreased the defocus aberration over the full spectral range.

### 3. Performance evaluation

The total energy resolution can be expressed as the vector sum of the main individual contributions: slit width, optical aberrations, and figure slope error of the grating and M1. We shall describe the slit width for an energy resolution of  $10^{-4}$ . Then we shall discuss each contribution to the total energy resolution.

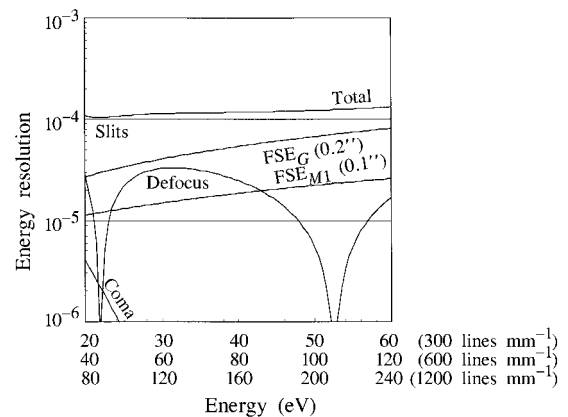
To keep the energy resolution defined by the slits constant, we calculate the corresponding slit width to give a resolution of  $10^{-4}$  (Shigemasa *et al.*, 1995). Fig. 2 shows the energy dependence of the entrance slit width and exit slit width to obtain an energy resolution of  $10^{-4}$  for the contribution of the slit width.

Fig. 3 shows the resolving power obtainable with this configuration using varied-line-spacing plane gratings. The widths of the entrance slit and the exit slit are defined to keep the slit contribution for the resolution as  $10^{-4}$ . Defocus aberration is negligible near the optimized energies, 22 eV and 52.5 eV. The contribution of figure slope error for total energy resolution is larger at higher photon energy. By considering these degradation parameters, the total energy resolution is  $1.2 \times 10^{-4}$  at maximum, indicating that the energy resolution of  $10^{-4}$  is almost achieved.



**Figure 2**  
Energy dependence of the entrance and exit slit width for an energy resolution of  $10^{-4}$  by the slit contribution.

The photon flux at the sample position is calculated as the product of four factors: the geometrical transmission factor, the reflectivity of optical elements, the grating diffraction efficiency and the photon flux at the source. To estimate the final photon flux we calculate each term as follows. First, the geometrical transmission factor of the optics was calculated by the ratio of the number of rays at the sample position and the number of rays at the source, as a result of a ray tracing simulation (Furukawa, 1996). Secondly, the reflectivity was calculated [see Centre for X-ray Optics (1997) and, for optical constants, Lynch & Hunter (1985)]. For this calculation the coating material of all the optical elements was Au, except for GC which was coated with Ni because it has a higher reflectivity in the region above 180 eV. Furthermore,  $s$  polarization was assumed for all optical elements, except for M0 for which  $p$  polarization was assumed. Surface roughnesses of 5 Å for mirrors and 10 Å for gratings were also assumed. The total reflectivity is calculated by the products of all mirrors and each grating. Thirdly, the grating diffraction efficiency was calculated using the formula for a lamellar-type grating (Frank *et al.*, 1975). Fourthly, the photon flux at the source was calculated using the formula derived by Yamamoto (1996). A photon flux of about  $10^{13}$  photons  $s^{-1}$  in a 0.01% bandwidth was obtained at the light source. From these values the photon flux at the sample position was obtained as shown in Fig. 4; it ranges from  $10^{10}$  to  $10^{11}$  photons  $s^{-1}$  (0.01% bandwidth) $^{-1}$ .



**Figure 3**

Total energy resolution considering the vector sum of the defocus aberrations, coma aberrations, figure slope error of the spherical mirror ( $FSE_{M1}$ ), figure slope error of the plane grating ( $FSE_G$ ), and entrance- and exit-slit contributions.

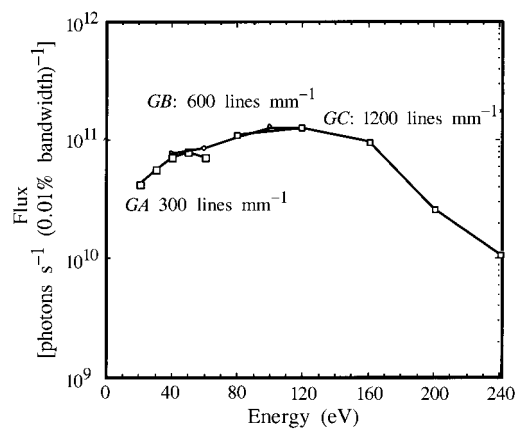


**Figure 4**

Photon flux at the sample *versus* energy.

The spot diagram at the sample position was obtained by ray-tracing simulation for 20 eV, where the spot is the broadest, because the exit slit is widest at 20 eV. The FWHM of the profile is 48  $\mu\text{m}$  for the vertical direction and 180  $\mu\text{m}$  for the horizontal direction.

#### 4. Conclusions

A beamline optical system is described that can provide high flux, high resolution and a wide energy range. The results of analytical calculation and ray-tracing simulation show that a resolving power of  $10^{-4}$  can be achieved for the full spectral range 20–240 eV. The estimated output photon flux ranges from  $10^{10}$  to  $10^{11}$  photons  $\text{s}^{-1}$  with a resolving power of  $10^{-4}$ . Furthermore, the beam size at the sample position is smaller than 0.2 mm (horizontal)  $\times$  0.05 mm (vertical). We have confirmed that the performance is sufficiently high to perform photoelectron spectroscopy with high resolving power by using Yan's design method (Yan & Yagishita, 1995), even if a bending-magnet light source with wide emittance is used.

We thank Professor Y. Yagishita and Dr H. Kato of the Photon Factory, KEK, and also thank Professor M. Oshima and Dr K.

Ono of the Graduate School of Engineering, The University of Tokyo, for valuable discussions.

#### References

- Amemiya, K., Kitajima, Y., Ohta, T. & Ito, K. (1996). *J. Synchrotron Rad.* **3**, 282–288.
- Centre for X-ray Optics (1997). *X-ray Interactions with Matter*, [http://www-cxro.lbl.gov/optical\\_constants/](http://www-cxro.lbl.gov/optical_constants/).
- Frank, A., Lindsey, K., Bennett, J. M., Speer, R. J., Turner, D. & Hunt, D. J. (1975). *Proc. R. Soc. London Ser. A*, **277**, 503–543.
- Furukawa, Y. (1996). *Ray Trace for Windows*, <http://okutsu.spring8.or.jp/RTW/toc.html>.
- Harada, T. & Kita, T. (1980). *Appl. Opt.* **19**, 3987–3993.
- Hettrick, M. C. & Underwood, J. H. (1988). US Patent 4 776 696.
- Koike, M., Beguiristain, R., Underwood, J. H. & Namioka, T. (1994). *Nucl. Instrum. Methods*, **A347**, 273–277.
- Lynch, D. W. & Hunter, W. R. (1985). *Handbook of Optical Constants of Solids*, edited by E. D. Palik, p. 290. Orlando: Academic Press.
- Shigemasa, E., Yan, Y. & Yagishita, A. (1995). KEK Report, 95–2. KEK, Tsukuba, Ibaraki 305, Japan.
- Yamamoto, S. (1996). *Sinkurotoron Housyakou No Kiso*, edited by H. Oyanagi, p. 127. Tokyo: Maruzen. (In Japanese.)
- Yan, Y. & Yagishita, A. (1995). KEK Report 95–9. KEK, Tsukuba, Ibaraki 305, Japan.